



Published in final edited form as:

Nature. 2010 March 4; 464(7285): 108–111. doi:10.1038/nature08738.

Hematopoietic stem cells derive directly from aortic endothelium during development

Julien Y. Bertrand^{1,2,5}, Neil C. Chi^{3,4,5}, Buyung Santoso^{1,2}, Shutian Teng^{1,2}, Didier Y. R. Stainier⁴, and David Traver^{1,2}

¹ Department of Cellular and Molecular Medicine, University of California, San Diego, La Jolla, CA 92093-0380

² Section of Cell and Developmental Biology, University of California, San Diego, La Jolla, CA 92093-0380

³ Department of Medicine, University of California, San Diego, La Jolla, CA 92093-0380

⁴ Department of Biochemistry and Biophysics, University of California, San Francisco, San Francisco, CA 94158

Abstract

A major goal of regenerative medicine is to instruct formation of multipotent, tissue-specific stem cells from induced pluripotent stem cells (iPSCs) for cell replacement therapies. Generation of hematopoietic stem cells (HSCs) from iPSCs or embryonic stem cells (ESCs) is not currently possible, however, necessitating a better understanding of how HSCs normally arise during embryonic development. We previously showed that hematopoiesis occurs through four distinct waves during zebrafish development, with HSCs arising in the final wave in close association with the dorsal aorta. Recent reports have suggested that murine HSCs derive from hemogenic endothelial cells (ECs) lining the aortic floor^{1,2}. Additional *in vitro* studies have similarly suggested that the hematopoietic progeny of ESCs arise through intermediates with endothelial potential^{3,4}. In this report, we have utilized the unique strengths of the zebrafish embryo to image directly the birth of HSCs from the ventral wall of the dorsal aorta. Utilizing combinations of fluorescent reporter transgenes, confocal timelapse microscopy and flow cytometry, we have identified and isolated the stepwise intermediates as aortic hemogenic endothelium transitions to nascent HSCs. Finally, using a permanent lineage tracing strategy, we demonstrate that the HSCs generated from hemogenic endothelium are the lineal founders of the adult hematopoietic system.

Precisely how the first HSCs are generated in the vertebrate embryo has been a matter of controversy for several decades. Recent studies have strongly supported the postulate of hemogenic endothelium, ECs that transiently possess the ability to generate HSCs during

Users may view, print, copy, download and text and data- mine the content in such documents, for the purposes of academic research, subject always to the full Conditions of use: http://www.nature.com/authors/editorial_policies/license.html#terms

⁵These authors contributed equally.

Author contributions

JYB, NCC and DT designed experiments. JYB and DT wrote the manuscript, with key input from NC and DYRS. JYB performed experiments. BS and ST generated and characterized the *factin:switch* reporter line. NCC and DYRS generated *kdrl:Cre*, and *kdrl:memCherry* transgenic lines.

vertebrate development⁵. By targeting expression of the Cre recombinase specifically to cells of the vasculature, Zovein et al. showed, using floxed reporter genes, that HSCs were generated from *Cdh5*⁺ (also referred to as VE-Cadherin) precursors, suggesting that HSCs arise from endothelium or shared endothelial precursors¹. Furthermore, experiments utilizing an inducible *Cdh5:Cre*^{ERT2} transgene suggested that ECs within the region flanked by the aorta, gonads and mesonephros (AGM) in the midgestation mouse embryo contained the majority of HSC potential¹. In addition, conditional deletion of the *Runx1* transcription factor gene in *Cdh5*⁺ cells led to loss of HSCs, suggesting that *Runx1* function is key in the transition from endothelium to HSC². *In vitro* studies have also suggested that ESC derivatives can generate hematopoietic cells through hemogenic endothelial intermediates^{3,4,6}. It remains to be determined, however, which regions of the embryo, or extraembryonic tissues, possess endothelium with hemogenic potential.

The appearance of cells having HSC characteristics has been observed in close association with arterial endothelium^{5,7}. In particular, the ventral floor of the dorsal aorta (DA) has been suggested by a number of investigators to be the primary birthplace of HSCs⁸. In the zebrafish embryo, we⁹ and others¹⁰ previously demonstrated that expression of a *cmyb:eGFP* transgene marks nascent HSCs along the ventral aspect of the DA between 28–48 hpf. To determine whether these cells arise directly from vascular precursors, we generated *cmyb:eGFP; kdrl:memCherry*¹¹ double transgenic animals and performed confocal timelapse imaging. Between 28–32 hpf, expression of the *kdrl* transgene (also known as *flkl1* and *vegfr2*) within the zebrafish equivalent of the AGM region is localized to the aorta, vein and developing intersomitic vessels; hematopoietic expression of the *cmyb* transgene initiates in cells along the DA around this time (Figure 1a,b). Four-dimensional imaging demonstrated that *cmyb:eGFP*⁺ cells arose directly from *kdrl:memCherry*⁺ cells specifically along the ventral aspect of the DA (Supplemental Movies 1, 2). As shown in Figure 1, *kdrl:memCherry*⁺ ECs displaying typical flattened morphology were occasionally observed to transform into spherical shapes, forming buds that extended into the lumen of the DA. By virtue of the membrane-specific expression of mCherry, buds were observed to initiate as *kdrl*⁺*cmyb*⁻ cells transitioned to *kdrl*⁺*cmyb*⁺ cells (Figure 1). In contrast to the proposed budding of mammalian HSCs into aortic circulation⁵, we almost always observed HSCs to migrate ventrally towards the caudal vein (CV; Supplementary Movies 1, 2). This is consistent with the observations of Kissa et al.¹², which suggested that AGM HSCs enter circulation via the dorsal wall of the CV in the zebrafish.

To confirm the hematopoietic nature of these budding AGM cells, we performed flow cytometry on dissociated *kdrl:RFP*¹³; *cmyb:eGFP* embryos at 36 hpf, the timepoint at which we observed the peak in number of *kdrl*⁺*cmyb*⁺ cells. Embryos were dissected to separate anterior, head tissues from the posterior trunk/tail region that contains the AGM. In accordance with our microscopic observations, no *kdrl*⁺*cmyb*⁺ cells were observed in anterior regions (Figure 2a) above background. By contrast, 0.25% of posterior cells were *kdrl*⁺*cmyb*⁺ cells (Figure 2b). We thus reasoned that these double positive cells represented the nascent HSCs observed in our imaging experiments (Figure 2c). *kdrl*⁺*cmyb*⁺ cells could be subdivided based upon differing levels of the *cmyb:eGFP* transgene (Figure 2b); each subset, along with single positive posterior fractions were highly purified by FACS and

queried for expression of hematopoietic and vascular genes by qPCR. As expected, expression of endothelial genes, including *kdrl*, *cdh5*, and *lmo2*, were highly expressed in *kdrl⁺cmyb⁻* cells (Figure 2d). In general, early *kdrl⁺cmyb^{lo}* precursors maintained similar expression levels of these vascular markers. As *cmyb:eGFP* levels increased in maturing *kdrl⁺cmyb⁺* cells, however, expression of most endothelial genes dropped dramatically. By contrast, expression of *cd41*, one of the earliest markers of mesodermal commitment to definitive hematopoiesis^{14,15}, initiated in *kdrl⁺cmyb⁻* cells and increased as *kdrl⁺* cells became *cmyb⁺* (Figure 2d). We observed little to no *cd45* expression in either *kdrl⁺cmyb⁻* or *kdrl⁺cmyb^{lo}* cells. As these precursors matured, however, we observed concomitant upregulation of *cd45* in *kdrl⁺cmyb⁺* and *kdrl⁻cmyb⁺* subsets (Figure 2d). These results are consistent with findings in the mouse. On embryonic day 10, murine AGM HSCs do not express CD45 (encoded by *ptprc*)^{14,15}. By day 11, however, embryonic HSCs become CD45⁺^{14,15}. Collectively, these results support the hypothesis that the *kdrl⁺cmyb⁺* cells observed to arise from the ventral wall of the DA are definitive hematopoietic precursors.

In order to trace the progeny of ECs in the zebrafish embryo, we employed an indelible marking system utilizing a floxed reporter transgene and a Cre driver that is specific to endothelium via *kdrl* upstream promoter/enhancer elements¹⁶. In the zebrafish, there exist two orthologues of the mammalian *flk1* gene, *kdr* and *kdrl*. The former exhibits a pan mesodermal expression pattern¹⁷, whereas *kdrl* and *Tg(kdrl:Cre)^{s898}* (Supplementary Figure 1) is expressed only in endothelium in a manner nearly identical to that of the murine *cdh5* gene^{18,19}. Thus, the *Tg(kdrl:Cre)^{s898}* line used in our studies mimics the *cdh5:Cre* knock-in mouse line employed in previous studies^{1,2}. We crossed *kdrl:Cre* animals to animals carrying a *Tg(βactin2:loxP-STOP-loxP-DsRed-express)^{sd5}* “switch” reporter transgene in which 10.5kb of upstream βactin promoter/enhancer sequence is followed by a 5.7kb floxed “superstop” cassette. Immediately downstream is a DsRed^{express} gene that serves as a reporter for Cre-based removal of the superstop cassette. As presented in Supplementary Figure 2, reporter gene expression was never observed in the absence of Cre, and induction of Cre in 24 hpf embryos led to stable reporter expression within nearly all hematopoietic cells for one year.

To test whether the *kdrl⁺; cmyb⁺* hematopoietic precursors observed in the AGM are *bona fide* HSCs, we generated *kdrl:Cre; switch* animals for long-term studies. Compared to whole kidney marrow (WKM) isolated from single transgenic *switch* animals that showed no expression of DsRed (Figure 3a), double transgenic *kdrl:Cre; switch* animals showed the vast majority of leukocytes to be labeled at six months of age (Figure 3b, c). Analysis of a large cohort of double transgenic animals showed that over 90% of WKM cells were marked at 3 months of age (Figure 3b). At 6 months of age, over 96% of WKM myeloid cells expressed the DsRed^{express} lineage tracer (Figure 3c). Since this cellular subset is comprised of over 90% neutrophils, which are characterized by lifespans restricted to a few days, this result suggests that the vast majority of, if not all, HSCs were marked by the *kdrl:Cre* transgene during their embryonic formation. Finally, marked WKM was sorted by DsRed expression level and subjected to qPCR for lineage-affiliated genes. As presented in Figure 3d, *pax5* (B lymphocyte-affiliated) and *pu.1* (myeloid-affiliated) expressing cells were contained within DsRed^{high} cells, and *gatal* expressing cells within the DsRed^{low} fraction.

These data are consistent with our previous demonstration that the β actin promoter is highly expressed in leukocytes, but is silenced upon erythropoietic differentiation²⁰. Thus, lineage tracing of *kdr1*⁺ hemogenic endothelium demonstrates robust, multilineage, long-term population of the adult hematopoietic organ. Furthermore, since expression of *kdr1* is rapidly extinguished as HSCs arise from hemogenic endothelium (Figure 2d), and since *kdr1*⁺*cmyb*⁺ transitional intermediates were no longer detectable in larval or adult stages (Supplementary Figure 3), our lineage tracing results support the hypothesis that HSCs no longer arise *de novo* following their specification in the embryo.

In summary, our imaging and lineage tracing studies demonstrate that the first HSCs born in the zebrafish embryo arise directly from hemogenic endothelium lining the ventral wall of the DA. These results complement previous studies in the avian²¹, amphibian²², and mammalian embryo^{1,2,7} and suggest that the cellular mechanisms of HSC generation have been highly conserved across vertebrate evolution. The finding that HSC development requires transition through a hemogenic endothelial intermediate should aid efforts to instruct HSC formation *in vitro* from pluripotent precursors, a necessity for therapies designed to replace the adult blood cell lineages.

Methods Summary

Tg(kdr1:HsHRAS-mCherry)^{s896} animals (referred to as *kdr1:memCherry* for clarity) were previously described¹¹. *Tg(kdr1:Cre)^{s898}* and *Tg(β actin2:loxP-STOP-loxP-DsRed-express)^{sd5}* adults were mated, and their progeny screened for the presence of DsRed⁺ vasculature at 48 hpf. Positive embryos were raised to adulthood; some were sacrificed to analyze WKM at several ages (7 weeks to 6 months) by flow cytometry. Flow cytometry was performed as described⁹, and sytox was used as a vital dye to exclude dead cells. Imaging was performed on an SP5 deconvolution confocal microscope (Leica, Germany). For time-lapse imaging, double transgenic *Tg(kdr1:HsHRAS-mCherry)^{s896}; Tg(cmyb:eGFP)* embryos were first screened for fluorescence, then anesthetized in tricaine and embedded in agarose. Time-lapse imaging was usually performed between 22 hpf and 36 hpf, in an environmental chamber maintained at 28°C. Raw data was analyzed using Volocity software (Improvision, Lexington, MA), and exported in Quicktime format.

Methods

Zebrafish husbandry

Zebrafish strains AB*, *Tg(kdr1:HsHRAS-mCherry)^{s896}*⁽¹¹⁾, *Tg(kdr1:RFP)^{la4}*⁽¹³⁾, *Tg(cmyb:eGFP)*⁽¹⁰⁾, *Tg(hsp70l:Cre)^{zf36}*⁽²³⁾, *Tg(kdr1:Cre)^{s898}*, and *Tg(β actin2:loxP-STOP-loxP-DsRed-express)^{sd5}* were mated, staged and raised as described²⁴, and maintained according to UCSD IACUC guidelines.

Generation of transgenic animals

Tg(kdr1:Cre)^{s898} transgenic animals were generated following cloning of a 6.8kb fragment of *kdr1* promoter/enhancer sequences²⁵ upstream of a promoterless Cre construct. The construct was cloned into the pIsceI meganuclease vector. We injected 200 pg of linearized DNA into one cell-stage transgenic reporter embryos; founders were identified by screening

for fluorescent progeny. Three *Tg(kdrl:Cre)* founders were recovered with identical expression patterns but varying levels. *Tg(kdrl:Cre)^{s898}* exhibited the strongest expression; this line was employed for these studies. *Tg(βactin2:loxP-STOP-loxP-DsRed-express)^{sd5}* transgenic animals were generated as follows: A loxP-flanked transcriptional STOP cassette, which contains four SV40 late polyadenylation signals in tandem, was excised from pBS.DAT-LoxStop vector²⁶ and ligated upstream of the fluorescent gene in the pDsRed-Express-1 vector (Clontech, Mountain View, CA). A 10.5 kb fragment immediately upstream of the *βactin2* translation start site was cloned by PCR in three fragments and sequentially ligated upstream of the STOP cassette. The 5' boundary of the fragment is 5'-GGTAGAGCCTTACATTTCTTCGTATTCTCA-3'. The transgenic construct was then excised and ligated into a Tol2 transgenesis vector²⁷. The resulting construct was co-injected with Tol2 mRNA into one-cell stage embryos to generate transgenic founders.

Flow cytometry

Embryos were collected at desired stages of development and anesthetized in E3 medium containing 0.1 mg/ml tricaine (Sigma). Disaggregation into single-cell suspension was achieved as previously described⁹. Juveniles and adults were sacrificed at 7 weeks to 6 months, and WKM was dissected and mechanically resuspended to obtain single-cell suspensions. Flow cytometric acquisitions were performed on a FACS LSR II (Becton Dickinson, San Jose, CA), and cell sorting was performed on a FACS ARIA (BD, San Jose, CA). Analyses were performed using FlowJo software (Treestar, Ashland, OR).

RNA isolation and QPCR

RNA was isolated from sorted cells using an RNAeasy kit (Qiagen, Valencia, CA), and cDNA was obtained using the qscript cDNA super mix (Quanta Biosciences, Gaithersburg, MD). QPCR reactions were performed using the Mx3000P® QPCR system (Stratagene, La Jolla, CA) according to the manufacturer's instructions (Stratagene). Biological triplicates were compared for each subset. For each independent experiment, elongation-factor-1-alpha (*eF1α*) expression was scored for each population. The signals detected for each transcript of interest were then normalized to *eF1α*, data were analyzed by the Ct method according to manufacturer's recommended protocol (Stratagene), then normalized to expression in WKM that was defined as 100% for all analyses, except for *hbae1* where 8–12ss *kdrl*⁺ cells were used as the reference. Primers were designed with Primer3 software²⁸. Primers: *cdh5-for*: TTCAAGAATCCTGTCATTGG, *cdh5-rev*: ATGTGCTGTAACCTGGAATG, *kdrl-for*: CTCCTGTACAGCAAGGAATG, *kdrl-rev*: ATCTTTGGGCACCTTATAGC; primers for *lmo2*, *cd41*, *cd45*, and *runx1* were described previously⁹.

Fluorescent microscopy and time-lapse imaging

Embryos were imaged using a Leica SP5 inverted confocal microscope (Leica, Germany). GFP, DsRed and mCherry were excited by 488, 543 and 594 nm laser lines, respectively. For time-lapse imaging, embryos were embedded in agarose (0.7% in E3 medium) containing Tricaine anaesthetic at a temperature of 30°C. Z-stacks were taken every 3 to 5 minutes. Movies were created following processing with Volocity software (Improvision, Lexington, MA).

Supplementary Material

Refer to Web version on PubMed Central for supplementary material.

Acknowledgments

We thank S. Lin for providing *kdr1:RFP* animals. JYB was supported by the Irvington program of the Cancer Research Institute and by the California Institute for Regenerative Medicine (CIRM), NCC by National Institutes of Health (NIH) HL074891, a Research and Education Foundation Award from GlaxoSmithKline and a Beginning Grant in Aid Award from the American Heart Association, BS by NIH F32DK752433, DYRS by the Packard Foundation and NIH HL54737, and DT by a Scholar Award from the American Society of Hematology, a New Investigator Award from CIRM, and NIH DK074482.

References

1. Zovein AC, et al. Fate tracing reveals the endothelial origin of hematopoietic stem cells. *Cell Stem Cell*. 2008; 3:625–636. [PubMed: 19041779]
2. Chen MJ, Yokomizo T, Zeigler BM, Dzierzak E, Speck NA. Runx1 is required for the endothelial to haematopoietic cell transition but not thereafter. *Nature*. 2009; 457:887–891. [PubMed: 19129762]
3. Eilken HM, Nishikawa S, Schroeder T. Continuous single-cell imaging of blood generation from haemogenic endothelium. *Nature*. 2009; 457:896–900. [PubMed: 19212410]
4. Lancrin C, et al. The haemangioblast generates haematopoietic cells through a haemogenic endothelium stage. *Nature*. 2009; 457:892–895. [PubMed: 19182774]
5. Cumano A, Godin I. Ontogeny of the hematopoietic system. *Annual review of immunology*. 2007; 25:745–785.
6. Murry CE, Keller G. Differentiation of embryonic stem cells to clinically relevant populations: lessons from embryonic development. *Cell*. 2008; 132:661–680. [PubMed: 18295582]
7. de Bruijn MF, Speck NA, Peeters MC, Dzierzak E. Definitive hematopoietic stem cells first develop within the major arterial regions of the mouse embryo. *The EMBO journal*. 2000; 19:2465–2474. [PubMed: 10835345]
8. Dzierzak E, Speck NA. Of lineage and legacy: the development of mammalian hematopoietic stem cells. *Nature immunology*. 2008; 9:129–136. [PubMed: 18204427]
9. Bertrand JY, Kim AD, Teng S, Traver D. CD41+ cmyb+ precursors colonize the zebrafish pronephros by a novel migration route to initiate adult hematopoiesis. *Development*. 2008; 135:1853–1862. [PubMed: 18417622]
10. North TE, et al. Prostaglandin E2 regulates vertebrate haematopoietic stem cell homeostasis. *Nature*. 2007; 447:1007–1011. [PubMed: 17581586]
11. Chi NC, et al. Foxn4 directly regulates *tbx2b* expression and atrioventricular canal formation. *Genes & development*. 2008; 22:734–739. [PubMed: 18347092]
12. Kissa K, et al. Live imaging of emerging hematopoietic stem cells and early thymus colonization. *Blood*. 2008; 111:1147–1156. [PubMed: 17934068]
13. Huang H, Zhang B, Hartenstein PA, Chen JN, Lin S. Nxt2 is required for embryonic heart development in zebrafish. *BMC Dev Biol*. 2005; 5:7. [PubMed: 15790397]
14. Mikkola HK, Fujiwara Y, Schlaeger TM, Traver D, Orkin SH. Expression of CD41 marks the initiation of definitive hematopoiesis in the mouse embryo. *Blood*. 2003; 101:508–516. [PubMed: 12393529]
15. Bertrand JY, et al. Characterization of purified intraembryonic hematopoietic stem cells as a tool to define their site of origin. *Proceedings of the National Academy of Sciences of the United States of America*. 2005; 102:134–139. [PubMed: 15623562]
16. Jin SW, Beis D, Mitchell T, Chen JN, Stainier DY. Cellular and molecular analyses of vascular tube and lumen formation in zebrafish. *Development*. 2005; 132:5199–5209. [PubMed: 16251212]
17. Bussmann J, Bakkers J, Schulte-Merker S. Early endocardial morphogenesis requires *Scf/Tal1*. *PLoS genetics*. 2007; 3:e140. [PubMed: 17722983]

18. Liao W, et al. The zebrafish gene *cloche* acts upstream of a *flk-1* homologue to regulate endothelial cell differentiation. *Development*. 1997; 124:381–389. [PubMed: 9053314]
19. Choi J, et al. FoxH1 negatively modulates *flk1* gene expression and vascular formation in zebrafish. *Developmental biology*. 2007; 304:735–744. [PubMed: 17306248]
20. Traver D, et al. Transplantation and in vivo imaging of multilineage engraftment in zebrafish bloodless mutants. *Nature immunology*. 2003; 4:1238–1246. [PubMed: 14608381]
21. Jaffredo T, Gautier R, Eichmann A, Dieterlen-Lievre F. Intraaortic hemopoietic cells are derived from endothelial cells during ontogeny. *Development*. 1998; 125:4575–4583. [PubMed: 9778515]
22. Ciau-Uitz A, Walmsley M, Patient R. Distinct origins of adult and embryonic blood in *Xenopus*. *Cell*. 2000; 102:787–796. [PubMed: 11030622]
23. Feng H, et al. Heat-shock induction of T-cell lymphoma/leukaemia in conditional Cre/lox-regulated transgenic zebrafish. *British journal of haematology*. 2007; 138:169–175. [PubMed: 17593023]
24. Westerfield, M. *The zebrafish book: A guide for the laboratory use of zebrafish (Brachydanio rerio)*. 2.1. University of Oregon Press; 1994.
25. Beis D, et al. Genetic and cellular analyses of zebrafish atrioventricular cushion and valve development. *Development*. 2005; 132:4193–4204. [PubMed: 16107477]
26. MacPherson D, et al. Cell type-specific effects of Rb deletion in the murine retina. *Genes & development*. 2004; 18:1681–1694. [PubMed: 15231717]
27. Kawakami K, et al. A transposon-mediated gene trap approach identifies developmentally regulated genes in zebrafish. *Developmental cell*. 2004; 7:133–144. [PubMed: 15239961]
28. Rozen, S.; Skaletsky, HJ. *Bioinformatics Methods and Protocols: Methods in Molecular Biology*. Humana Press; 2000. Primer3 on the WWW for general users and for biologist programmers; p. 365-386.

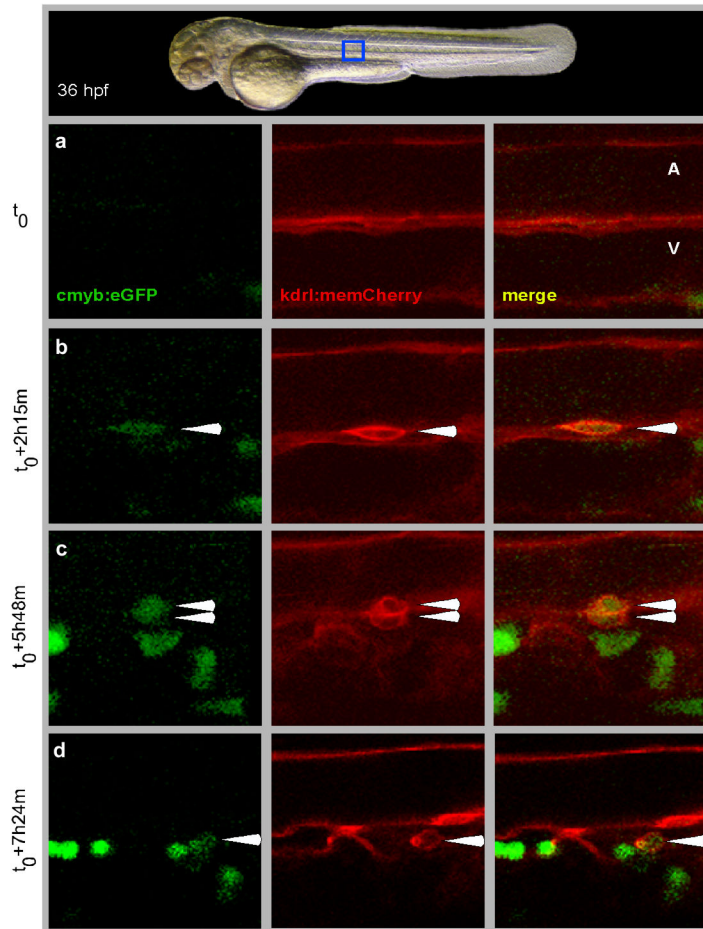


Figure 1. Direct imaging of HSC emergence from the embryonic aortic floor
a–d, Time-lapse imaging of a double transgenic *cmyb:eGFP*, *kdrl:memCherry* embryo between 30–38 hpf. Four sequences from Supplementary video 1 are presented, documenting the stepwise emergence of HSCs from hemogenic endothelium in denoted region (blue box, upper panel). For each time point, the GFP, memCherry and merged images are shown. memCherry; GFP double positive cells are denoted by white arrowheads (A, aorta; V, vein).

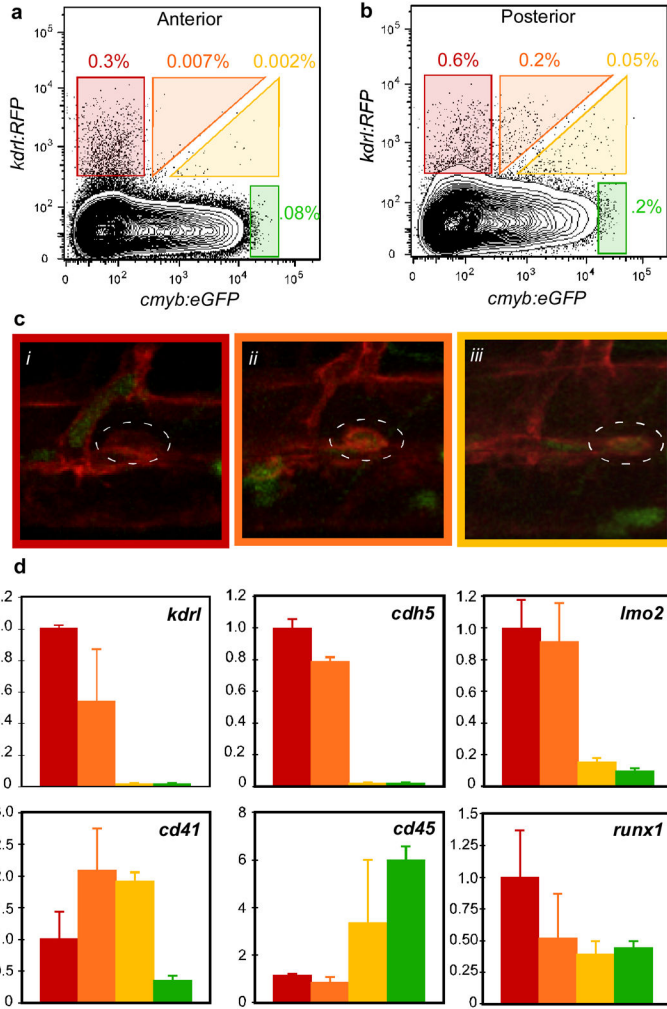


Figure 2. Prospective isolation of aortic hemogenic endothelium and nascent HSCs
a–b, Double transgenic *cmyb:eGFP; kdr1:RFP* embryos were dissected to separate anterior from posterior, AGM containing tissues at 36 hpf. Throughout the figure, the cellular fraction including hemogenic endothelium is denoted by red boxes or bars, nascent HSCs by orange boxes or bars, maturing HSCs by yellow boxes or bars, and mature HSCs by green boxes or bars. **c**, Correlation of FACS expression profiles to stepwise HSC emergence in *kdr1:memCherry; cmyb:eGFP* embryos (*i*, hemogenic endothelium; *ii*, nascent HSC; *iii*, maturing HSC). Images captured from Supplementary video 1. **d**, Quantitative PCR expression for endothelial (top panel) and hematopoietic (bottom panel) genes in purified *kdr1+cmyb-* (red), *kdr1+cmyb^{lo}* (orange), *kdr1^{lo}cmyb+* (yellow) and *kdr-cmyb+* cells (green). Units on Y-axis represent fold changes from the *kdr1+cmyb-* reference standard, which is set at 1.0. We note that the *kdr-cmyb+* population contains some neuronal cells, effectively diluting the vascular and hematopoietic signals. Error bars, standard deviation.

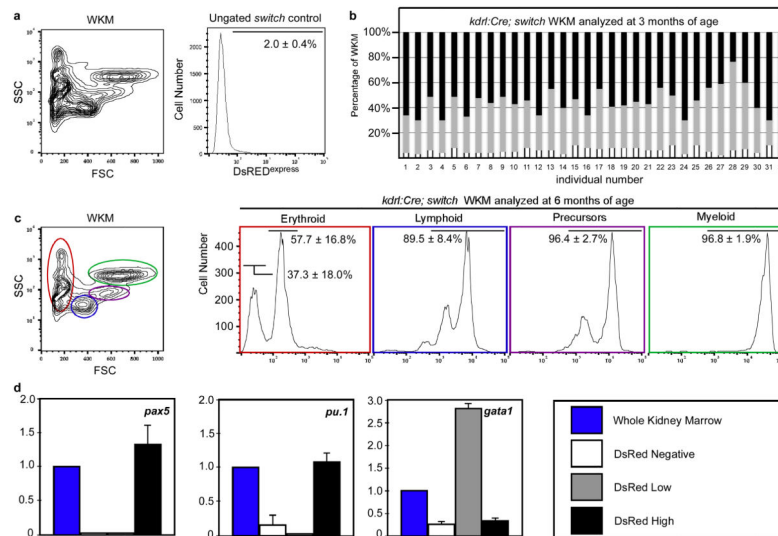


Figure 3. Long-term lineage tracing of embryonic endothelial cells

a, Flow cytometric analysis of WKM from a transgenic *βactin:switch* adult animal. **b**, Bar graphs show the percentage of switched cells (DsRed^{hi} shaded black; DsRed^{lo} grey) in WKM of double transgenic *kdrl:Cre; βactin:switch* adult animals (n=32). DsRed⁻ cells are represented in white. **c**, Histogram plots show percentages of switched hematopoietic lineages at 6 months of age in WKM (average ± standard deviation, n=5). **d**, Quantitative PCR expression of switched (DsRed^{hi} in black; DsRed^{lo} in grey) and non-switched cells (white bars) at 3 months, for B lymphoid (*pax5*), myeloid (*pu.1*) and erythroid (*gata1*) genes. Units on Y-axis represent fold changes from WKM, the reference standard set at 1.0. Error bars, standard deviation.